

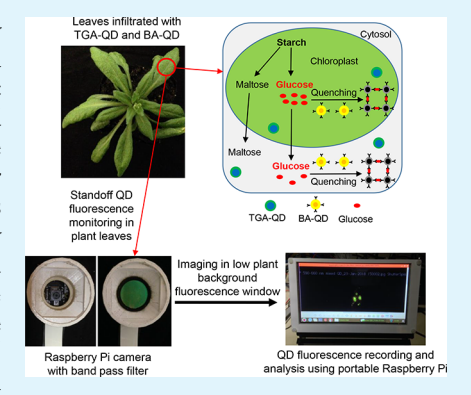
# Standoff Optical Glucose Sensing in Photosynthetic Organisms by a **Quantum Dot Fluorescent Probe**

Jinming Li,†,‡ Honghong Wu,‡ Israel Santana, Mackenzie Fahlgren, and Juan Pablo Giraldo\*®

Department of Botany and Plant Sciences, University of California, Riverside, California 92521, United States

Supporting Information

ABSTRACT: Glucose is a major product of photosynthesis and a key energy source for cellular respiration in organisms. Herein, we enable in vivo optical glucose sensing in wild-type plants using a quantum dot (QD) ratiometric approach. The optical probe is formed by a pair of QDs: thioglycolic acid-capped QDs which remain invariable to glucose (acting as an internal fluorescent reference control) and boronic acid (BA)-conjugated QDs (BA-QD) that quench their fluorescence in response to glucose. The fluorescence response of the QD probe is within the visible light window where photosynthetic tissues have a relatively low background. It is highly selective against other common sugars found in plants and can be used to quantify glucose levels above 500 µM in planta within the physiological range. We demonstrate that the QD fluorescent probe reports glucose from single chloroplast to algae cells (Chara zeylanica) and plant leaf tissues ( Arabidopsis thaliana) in vivo via confocal microscopy and to a standoff Raspberry Pi camera setup. QD-based probes exhibit bright fluorescence, no photobleaching,



tunable emission peak, and a size under plant cell wall porosity offering great potential for selective in vivo monitoring of glucose in photosynthetic organisms in situ.

KEYWORDS: glucose, photosynthesis, nanosensors, non-contact detection, ratiometric approach

# 1. INTRODUCTION

Photosynthesis harvests and converts solar energy into carbohydrates such as starch<sup>1</sup> which are hydrolyzed at night into smaller sugar molecules, e.g., glucose<sup>2</sup> and maltose.<sup>3</sup> The glucose molecules are then converted into pyruvate for producing adenosine triphosphate by cellular respiration.<sup>4</sup> Glucose is a key signaling molecule in plants that regulates growth and developmental processes through complex intracellular signal transduction pathways. In higher plants, glucose has been implicated to be the primary sugar signal controlling seed germination, seedling vegetative growth, primary and lateral root growth, and leaf development. Despite its importance, there are no optical probes for the detection of glucose in vivo in wild-type photosynthetic organisms, limiting the study of photosynthesis, respiration, glucose signaling, and energy harvesting biomaterials. Furthermore, current methods to measure photosynthesis in vivo are based on carbon dioxide fixation 7-11 but not on the main photosynthetic product, that is, carbohydrates.

Previous approaches for in vivo glucose sensing in plants have been limited to genetically encoded molecular nanosensors in a handful of plant model species. 12 Bacterial periplasmic binding proteins (PBPs) allow the detection of a wide range of analyte concentrations in living cells. The PBP's hinge-bending movement in response to sugars leads to fluorescence changes via resonance energy transfer (FRET) between two coupled green fluorescent proteins. Although it is a successful approach to monitor glucose in plant tissues, the

FRET-based nanosensors are only available in genetically modified Arabidopsis<sup>13,14</sup> and rice. 15 Several nanoparticle (NNP)-based optical methods for sensing glucose are available for in vitro applications or in nonplant systems. For instance, 3-aminobenzeneboronic acid-functionalized graphene<sup>18</sup> and Ag<sub>2</sub>S quantum dots (QDs)<sup>19</sup> have been used for monitoring glucose in mammalian cells. However, these approaches have not been utilized for in vivo sensing of glucose in plants. A major challenge is that fluorescent pigments in photosynthetic tissues, including chlorophylls and carotenoids, introduce a strong background signal that limits the range of light wavelengths for optical glucose detection. Furthermore, unlike animal cells, plants have a cell wall with a porosity lower than 13 nm<sup>11</sup> which restricts the range of existent NNPs used as sensors for glucose. A NNP platform designed for in vivo glucose sensing in plants could be widely used across diverse plant taxa in the field.

QDs have attracted increasing interest as fluorescent probes owing to their bright fluorescence, photostability, continuous absorption spectra, and tunable emission. 20,21 QDs fluorescence quenching caused by mediated assembly of QDs by a small molecular analytes, such as glucose, has yielded a mean of fabricating QD arrays with tunable optical properties in response to concentration changes of analytes in living systems.

Received: May 2, 2018 Accepted: July 30, 2018 Published: July 30, 2018 Phenylboronic acid (PBA)-modified QDs have been shown to act as probes for intracellular glucose detection in cancer cells. This QD glucose probe has PBA-functionalized groups that serve as linkers to form stable boronate complexes with glucose cis-diols. Using a similar approach, QDs offer the potential for in vivo plant glucose sensing with the advantages of having: (1) smaller size than the maximum porosity of cell walls, (2) versatile surface chemistry allowing surface conjugation of functional groups for targeted delivery or biosensing within organelles, and (3) photostability with tunable and prolonged fluorescence intensity in vivo. (26,27)

Analyte detection in complex living systems such as photosynthetic organisms containing autofluorescent pigments can be challenging because of the interference of the probe with other molecules, scattering media, and changes in probe location within the detector focal plane. 28,29 Ratiometric detection approaches can control these factors in glucose sensing within photosynthetic living tissues and organelles using the ratio of two fluorescence emission intensities at different wavelengths. Ratiometric sensors have allowed conversion of plants into detectors of nitroaromatics<sup>30</sup> and monitoring hydrogen peroxide and nitric oxide (NO)<sup>31</sup> and in mammalian systems to detect pH,<sup>32</sup> oxygen,<sup>33</sup> and other analytes, for example, mechlorethamine. 34 Single-walled carbon nanotubes (SWCNTs) have been used as ratiometric sensors for in vivo monitoring of NO and hydrogen peroxide  $(H_2O_2)$  in plant photosynthetic tissues by recording the nearinfrared fluorescence response from two SWCNT electronic types having distinct emission peaks.<sup>31</sup> FRET-based sensors that monitor analytes in vivo have adopted a ratiometric approach because they are more stable to external noise and detection geometry in living systems.35 Current QD fluorescence-based probes for glucose are single wavelength intensity modulation-type probes. <sup>22,36</sup> Fluorescent QDs conjugated with BA have been used in this way to sense glucose in aqueous solution.3

Boronic acid (BA)-based fluorescent probes have been widely used for glucose sensing. 38,39 BA is a compound related to boric acid that reacts with 1,2-diols or 1,3-diols in aqueous solution to create five- or six-membered cyclic esters. Glucose detection by BA fluorescent probes is based on the interaction between surface BA group and glucose two pairs of rigid cis-diols. A tetraphenylethene-based fluorescent sensor modified with BA detects glucose by aggregation-induced changes in the probe fluorescence emission. Synthetic NNP-based fluorescent probes offer a tool to detect or sense glucose in vivo in diverse photosynthetic organisms and significantly advance photosynthesis and sugar signaling research. However, to our knowledge, there are no NNP-based optical sensors for glucose in vivo sensing in photosynthetic organisms.

Herein, we developed an in vivo standoff glucose probe for photosynthetic organisms based on QDs modified with BA-coated QDs (BA-QDs) and thioglycolic acid (TGA)-coated QDs (TGA-QDs) (Figure 1). The BA-QD fluorescence quenches in response to glucose, whereas the TGA-QD fluorescence remains invariant acting as an internal reference control. We demonstrate the concept of in vitro, in vivo, and optical standoff QD detection of glucose in photosynthetic model organisms including the algae (Chara zeylanica) and the land plant Arabidopsis thaliana. The QD probe has high selectivity for glucose based on the covalent binding between the two pairs of cis-diols of glucose and BA on the QD surface.

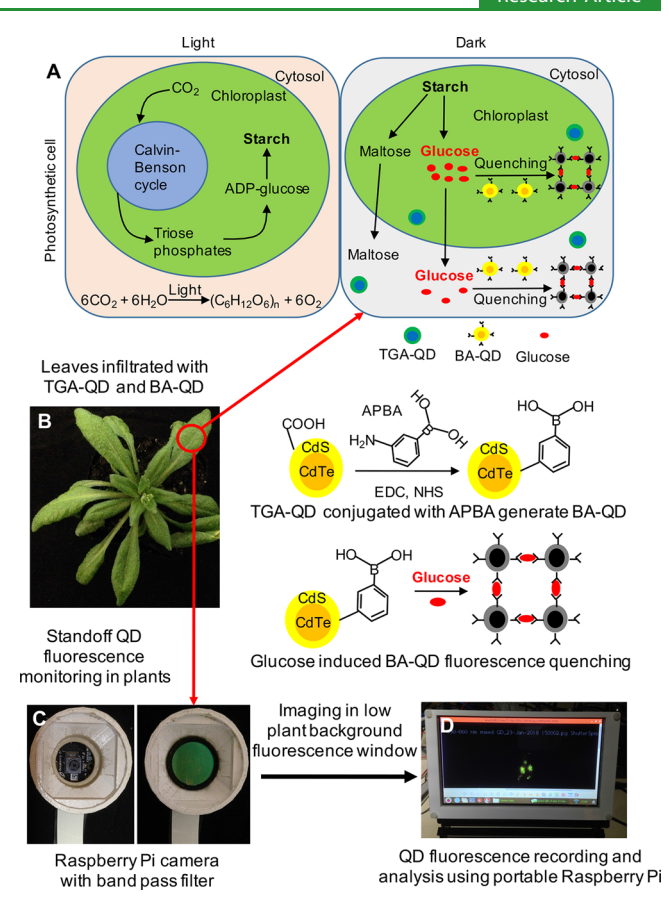


Figure 1. Schematic diagram of in vivo glucose sensing and standoff imaging by the QD fluorescent probe using a Raspberry Pi camera setup. (A) Glucose synthesis by chloroplasts in photosynthetic cells. Light energy is stored in chloroplasts as starch during daytime and then converted into glucose and maltose at night. (B) QD signals from dark adapted *Arabidopsis* leaves were monitored by two Raspberry Pi cameras equipped with (C) band pass optical filters for imaging the QD probe within a visible window of low leaf background. (D) Monitored QD fluorescence signal is recorded by a Raspberry Pi.

The detection range of the QD probe from 100 to 1000  $\mu$ M in vitro and from 500 to 1000  $\mu$ M in photosynthetic tissues and organelles in vivo is within the expected physiological range of light-grown plants. <sup>13,45</sup> NNP-based approaches for standoff optical monitoring of plant sugars will be a highly enabling tool to advance our understanding of plant photosynthesis, biofuels, sugar transport, and biomaterial research.

# 2. EXPERIMENTAL SECTION

**2.1. Materials.** Cadmium chloride hydrate (CaCl<sub>2</sub>), TGA (99%), NaBH<sub>4</sub> (96%), tellurium powder (99.8%), *N*-hydroxysuccinimide (NHS), *N*-(3-dimethylaminopropyl)-*N*′-ethylcarbodiimide hydrochloride (EDC), and 3-aminophenylboronic acid (APBA) were purchased from Sigma-Aldrich. Glucose, sucrose, fructose, lactose, maltose, and galactose were obtained from Fisher Scientific. The algae (*C. zeylanica*) (Carolina biological supply, catalog 162120) and fourweek old *A. thaliana* (Columbia 0) were grown in Adaptis 1000 growth chambers (Conviron) at 200  $\mu$ mol m<sup>-2</sup> s<sup>-1</sup> photosynthetic active radiation, 24 ± 1 °C, 60% humidity, and 14/10 h day/night regime. Plants were hand-watered with tap water once every two days. Tap water was replaced in the Algae medium once a week.

**2.2. Instruments.** The UV-vis absorption spectra were recorded by a Shimadzu UV-vis spectrophotometer UV-2600. The fluorescence emission spectra were measured by PTI QuantaMaster 400

(HORIBA Scientific Ltd) using 365 nm excitation for QDs. The FTIR spectra were recorded by Nicolet 6700 FTIR (Thermo Fisher Scientific). The dynamic light scattering (DLS) measurements were performed in a Zetasizer Nano Series from Malvern. The transmission electron microscopy (TEM) images were collected in FEI Tecnai12 at 120 kV voltage. The confocal images were collected in a Zeiss 510 microscope applying a 458 nm excitation for QDs, 514 nm for FM4-64, 633 nm for chloroplasts. The emission detection range was set at 480-520 nm for TGA-QD, 535-590 nm for BA-QD, 565-615 nm for FM4-64, and 685-750 nm for chloroplasts. The fluorescence intensity of confocal images was analyzed in ImageJ (NIH).

2.3. Synthesis of a QD Glucose Probe. The synthesis of TGAcapped CdTe/CdS QDs was performed as reported previously with some modifications.<sup>46</sup> First, NaHTe was prepared by adding 40 mg of NaBH<sub>4</sub> to a flask containing 23 mg of tellurium powder and 2 mL of Milli-Q water. The reaction was maintained for several hours until all of the tellurium powder was dissolved. CdCl<sub>2</sub> (9.2 mg, 0.5 mmol) and TGA (4.6 mg, 0.5 mmol) were dissolved in 100 mL of Milli-Q water, followed by adjustment of the pH to 11 (pH meter; Orion Star A211, Thermo Scientific) by the addition of 1 M NaOH solution. Then, freshly prepared NaTeH solution (0.062 mmol) was quickly injected into the mixture under vigorous stirring, followed by refluxing under open-air conditions. Thioacetamide (3.12 mL, 0.4 mM) as a sulfur source was added separately to the CdTe QD (100 mL) keeping a constant 1:1 S/Te molar ratio in the solution. Aliquots of the reaction solution were taken out at regular intervals for further photoluminescence (PL) and absorption characterization. Two TGA-ODs were synthesized: the TGA-QD (592 nm) for BA-QD synthesis and the TGA-QD (523 nm) were used as the reference QDs for glucose sensing in vitro and in vivo. For synthesizing the BA-QD, the TGA-QD (592 nm) was conjugated with APBA by the reaction between -NH<sub>2</sub> and -COOH.<sup>47</sup> Briefly, EDC (0.3 mL, 0.025 mM) and sulfo-NHS (0.2 mL, 0.015 mM) were added to the TGA-QD solution (10 mL, 100 nM) to activate carboxyl of QDs under stirring for 2 h. Then, the APBA (0.5 mL, 0.025 mM) was added to the TGA-QD solution and stirred for 4 h to form the BA-QD. The BA-QDs were collected by centrifugation. The synthesized TGA-QD (523 nm) and BA-QD were characterized by UV-vis, FTIR, and DLS.

2.4. Glucose Sensing by a QD Fluorescent Probe in Vitro. The fluorescence emission spectra were measured in separate solutions of 100 nM BA-QD and 100 nM TGA-QD in 2 mL 1× TES buffer (10 mM, pH 7.4) or mixed solutions (TGA-QD: 100 nM, BA-QD: 100 nM, 2 mL 1× TES buffer, 10 mM, pH 7.4) before and after 60 min incubation with glucose at different concentrations (0, 100, 200, 500, and 1000  $\mu$ M). Similarly, incubation time dependence of fluorescence emission measurements was performed at 0, 20, 40, 60, and 120 min after addition of glucose (1000  $\mu$ M).

The QD probe selectivity to sugars was determined in a mixed solution of TGA-QD (100 nM) and BA-QD (100 nM) in 2 mL 1× TES buffer (10 mM, pH 7.4). The fluorescence emission spectra of the QD glucose probe were measured before and after incubating with sugars (glucose, sucrose, fructose, lactose, maltose, and galactose,  $1000 \ \mu\text{M}$ ) for 60 min.

For characterization of BA-QD aggregation in the presence of glucose, DLS measurements were performed in BA-QD (100 nM) suspended in 2 mL 1× TES buffer (10 mM, pH 7.4) before and after adding glucose (1000  $\mu$ M) at incubation times from 0 to 120 min. The BA-QD solutions with and without glucose (1000  $\mu$ M, 60 min incubation) were imaged by TEM at 120 kV.

2.5. Glucose Sensing by a QD Fluorescent Probe in Vivo. Glucose detection in vivo was performed in algae of C. zeylanica and leaves of Arabidopsis plants incubated or infiltrated,<sup>48</sup> with the QD glucose probe suspended in TES buffer solution (TGA-QD 200 nM and BA-QD 200 nM in 2 mL 1× TES buffer, 10 mM, pH 7.4) and the cell membrane dye FM 4-64 (2 µg/mL) for 2 h. Because the QD fluorescent probe is developed for the detection of glucose in planta, the pH of the buffer (pH 7.4) is similar to that of the chloroplast stroma (pH  $7.5-7.9^{49}$ ) and the plant cell cytosol (pH  $7.4-7.\overline{5}^{50}$ ). The algae were washed with 1× TES buffer three times to remove the QDs that were not internalized and remained in solution. Glucose at

concentrations ranging from 0 to 1000  $\mu M$  was added to the algae medium. Leaf discs of Arabidopsis plants were incubated with glucose (1x TES buffer with 1000  $\mu$ M glucose). Confocal images were collected at 0, 20, 40, and 60 min.

2.6. In Vivo Standoff Glucose Imaging. Flat leaves from fourweek old Arabidopsis plants were infiltrated with 1000 µM glucose followed by infiltration with a newly prepared mixture of TGA-QD and BA-QD in TES buffer solution. After 0.5 h dark incubation, the abaxial leaf surface (infiltrated area) was set to face two Raspberry Pi cameras (Raspberry Pi NoIR Camera Module V2—8 MP, 1080P30) equipped with band pass filters (BP480-520 nm filter for TGA-QD fluorescence and BP590-660 nm filter for BA-QD fluorescence, Omega Optical, USA). Measuring time points were set at 0, 5, 10, 20, 30, 45, and 60 min. At each measurement, QDs in infiltrated leaves were excited by a 365 nm UV lamp (3UV—38 UV lamp, UVP, LLC) for 10 s and fluorescence images were collected through the Raspberry Pi camera setup. Except for the UV excitation at each measurement time point, plants were kept under dark. A comparison between leaves under dark and light (200  $\mu$ mol m<sup>-2</sup> s<sup>-1</sup>) conditions was also performed without addition of glucose.

2.7. Ratio Maps by ImageJ Analysis. Ratio maps of TGA-QD and BA-QD fluorescence intensity  $(F_{\rm TGA-QD}/F_{\rm BA-QD})$  in algae and Arabidopsis in response to glucose in vivo were generated in ImageJ (NIH). Briefly, TGA-QD and BA-QD fluorescence intensity images at the same time point were converted from RGB mode to 32-bit format in ImageJ. The converted images were further processed with a "Calculator Plus" function of ImageJ. After generating a new ratio map, a 16-color LUT format was applied to highlight the differences in glucose detection within photosynthetic tissues and organelles.

2.8. Colocalization Analysis. Colocalization analysis of QDs in A. thaliana leaf mesophyll cells infiltrated with TGA-QD and BA-QD glucose probes was performed using ImageJ software. Confocal images were splitted into TGA-QD, BA-QD, and chloroplasts channels by using the "Split channels" function in ImageJ. The COLOC2 analysis package on ImageJ was used to determine colocalization/overlapping rate between TGA-QD and BA-QD NNPs and its colocalization rate with chloroplasts. The Manders' coefficient comparing pixel by pixel was calculated 51,52 after subtracting the background from images using the "Subtract background" function in ImageJ.

**2.9. Cell Viability Staining.** Cell viability staining of the algae (*C.* zeylanica) and Arabidopsis (Col-0) leaves incubated with TGA-QD and BA-QD was performed using propidium iodide (PI, 1 mM, incubate 10 min; plant cell viability assay kit, PA0100, Sigma-Aldrich) and Hoechst 33342 (10  $\mu g/mL$ , incubate 10 min<sup>53</sup>), respectively. We used Hoechst 33342 to assess cell viability under the presence of BA-QD because PI fluorescence emission significantly overlaps with that of BA-QD and chloroplast autofluorescence in leaves. Briefly, algae and Arabidopsis leaves were incubated with TGA-QD and BA-QD after 24 h; then, algae cells and leaf discs were stained with either PI or Hoechst 33342 for 10 min. After rinsing in distilled water for three times, the stained samples were then mounted on microscopy slides for confocal microscopy (Leica SP5) as described in our previous publication.<sup>54</sup> The confocal imaging settings for TGA-QD-incubated leaves were 590-640 nm for PI and 700-800 nm for chloroplasts under laser excitation of 488 nm. The confocal imaging settings for BA-QD-incubated leaves were 420-510 nm for Hoechst 33342 and 700-800 nm for chloroplasts under laser excitation of 405 and 514 nm. Algae and Arabidopsis leaves incubated with buffer control without NNPs were used to determine background PI and Hoechst 33342 levels. The chlorophyll content of Arabidopsis leaves infiltrated with TGA-QD and BA-QD was monitored using a chlorophyll meter (SPAD 502, Konica Minolta, Japan).5

**2.10. Statistical Analysis.** All data were represented as mean ± SD (n = biological replicates) and analyzed using SPSS 23.0. Comparison was performed by independent sample *t*-test (two-tailed) or one-way ANOVA based on Duncan's multiple range test (twotailed). \* and \*\* represent P < 0.05 and P < 0.01, respectively.

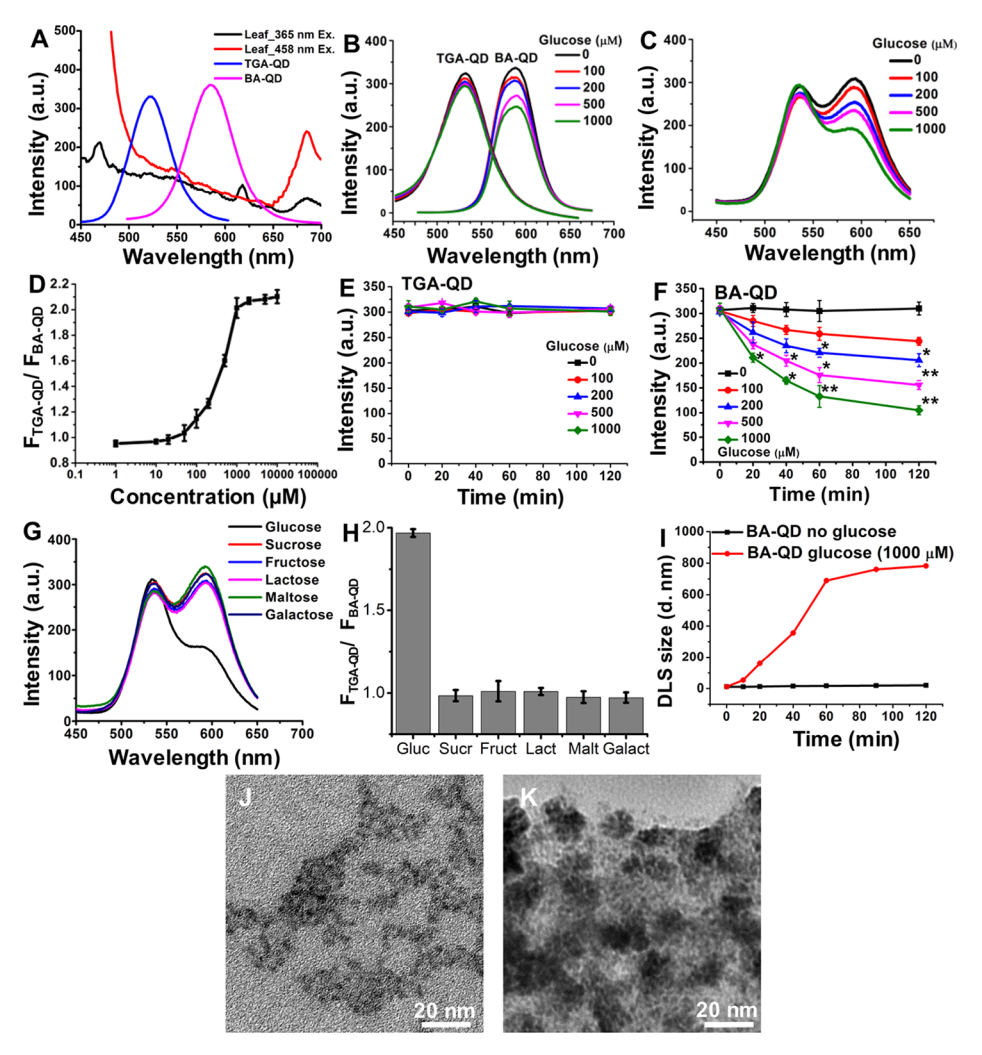


Figure 2. Detection of glucose in vitro by QD fluorescent probe and its selectivity against common plant sugars. (A) Fluorescence spectra of TGA-QD, BA-QD, and leaf background signal under 365 and 458 nm excitation. (B) TGA-QD fluorescence spectra remain relatively constant after adding glucose, whereas the BA-QD fluorescence quenches steadily in separate solutions or (C) combined QD using a ratiometric approach. (D) Ratio of fluorescence emission peak of TGA-QD and BA-QD fluorescence ( $F_{\text{TGA-QD}}/F_{\text{BA-QD}}$ ) in response to glucose. (E) In vitro temporal patterns of TGA-QD and (F) BA-QD fluorescence after adding glucose. Fluorescence spectra (G) and relative intensity changes (H) of the QD probe to glucose, sucrose, fructose, lactose, maltose, and galactose. BA-QD DLS size (I) and TEM images in response to glucose at 0 (J) and 1000 μM concentrations (K). Asterisks denote significance differences relative to no glucose (0 μM) (t-test). Scale bar: 20 nm.

### 3. RESULTS AND DISCUSSION

3.1. QD Glucose Probe Synthesis and Characterization. The TGA-QD and BA-QD forming the glucose probe were synthesized with a CdTe/CdS core/shell structure. TGA was used as a ligand<sup>56</sup> as it enhances the PL of QDs and stabilizes them in water solution by forming a shell structure of CdS. The carboxyl group in TGA can be conjugated to amino BAs (APBA) on the QD surface forming BA-QD. Leaves have a strong background fluorescence below 500 nm and above 650 nm<sup>S7</sup> (Figure 2A), and the FM 4-64 dye (ThermoFisher) used to label cell membranes in QD localization experiments of confocal microscopy has a significant fluorescence starting from 600 nm; therefore, we synthesized TGA-QD and BA-QD with significant fluorescence within this narrow visible window between 500 and 600 nm (Figure 2B). We synthesized TGA-QD as an internal reference control having a 523 nm peak of fluorescence emission to avoid the steep increase in background fluorescence of Arabidopsis leaves below 500 nm (Figure 2A). Similarly, we made BA-QD having a fluorescence peak of emission at 595 nm below the range of significant

fluorescence emission of FM 4-64. The UV–vis absorbance spectrum of TGA-QD and BA-QD shows a characteristic absorption spectrum of CdTe QD $^{58}$  having UV absorption from 350 to 550 nm (Figure S1A). The hydrodynamic diameter of TGA-QD and BA-QD was determined by DLS as 10.23  $\pm$  1.32 nm and 11.31  $\pm$  2.13 nm, respectively (Figure S1C). The BA-QD DLS size smaller than the cell wall porosity  $^{23}$  is ideal for the transport of the NNPs through plant cells.

**3.2.** Glucose Sensing in Vitro by a QD Fluorescent Probe. We characterized the concentration dependence of QD glucose probe fluorescence emission to glucose concentration  $(0-1000~\mu\mathrm{M})$ . The glucose-induced aggregation of BA-QD significantly quenches the fluorescence of the resultant QD assemblies (Figures 2B and S2A), whereas the TGA-QD remains invariant to glucose (Figures 2B and S2B). The added glucose leads to the aggregation of the BA-QD based on the covalent binding between the two pairs cis-diols of glucose and BA of the BA-QD surface, whereas the TGA-QD-COOH group does not react with the cis-diol group (Figure 1).  $^{22,36}$  As

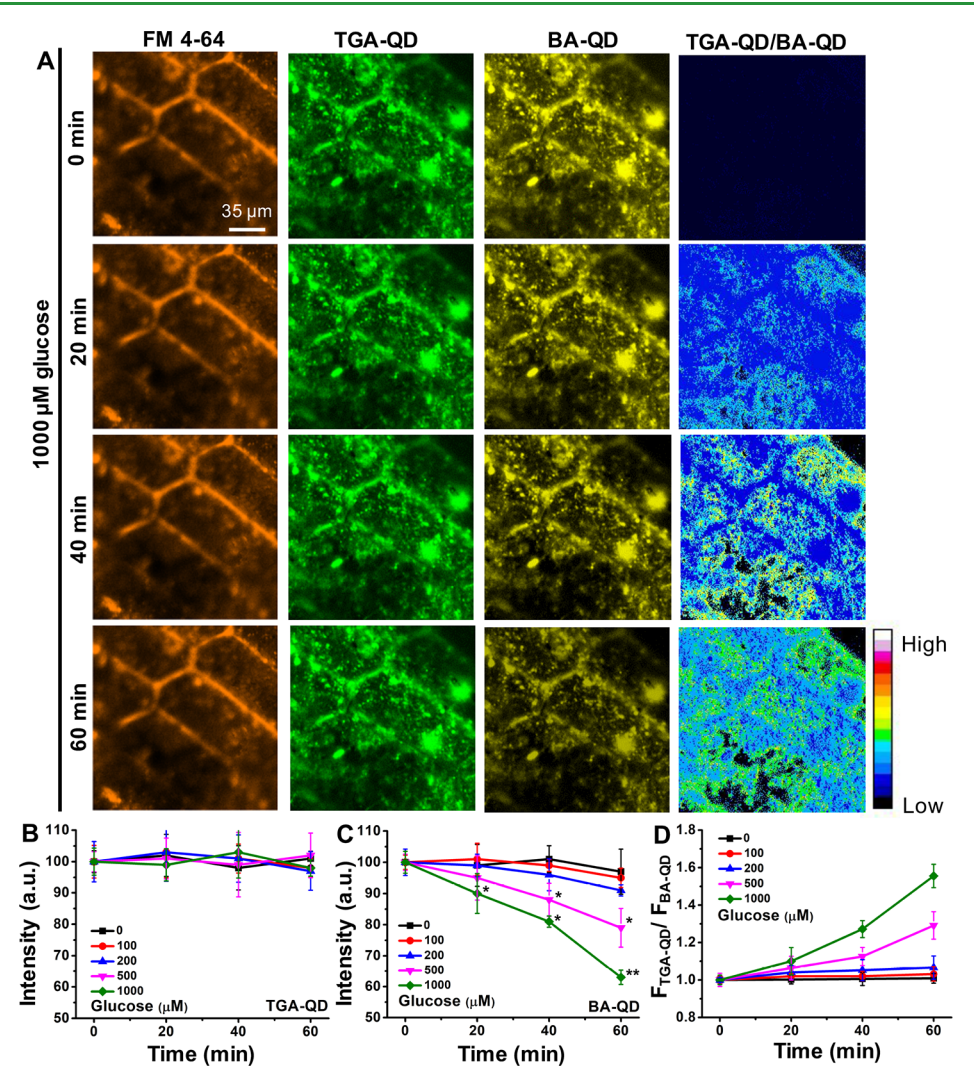


Figure 3. In vivo sensing of glucose in algae (*C. zeylanica*) by TGA-QD and BA-QD probes. (A) Confocal images of algae stained by FM 4-64 (orange, cell membrane) and incubated with TGA-QD (green) and BA-QD (yellow). In the presence of glucose (1000  $\mu$ M), the fluorescence intensity of TGA-QD remains relatively constant, whereas the fluorescence of BA-QD quenches steadily over time. Scale bar: 35  $\mu$ m. Temporal patterns of relative fluorescence intensity changes of TGA-QD (B) and BA-QD (C) after the addition of glucose to algae in vivo. (D) Changes in the ratio of TGA-QD and BA-QD fluorescence intensity ( $F_{TGA-QD}/F_{BA-QD}$ ) in response to glucose. Asterisks denote statistical significance relative to control (0  $\mu$ M glucose) (t-test).

expected, TGA-QD and BA-QD combined show that in the presence of glucose, the fluorescence emission of TGA-QD remains relatively constant, whereas the BA-QD fluorescence spectrum quenches steadily (Figure 2C). The BA-QD fluorescence quenching upon the addition of glucose (1000  $\mu$ M, in 10 mM pH 7.4 TES buffer) was partially recovered after adding glucose oxidase (10 U, in 10 mM pH 7.4 TES buffer), indicating the reversibility of BA-QD fluorescence response to glucose (Figures S2C and 2D). Glucose oxidase converts glucose to gluconolactone thus removing one of the pairs of cis-diols in glucose. Catalase (350 U, in 10 mM pH 7.4 TES buffer) was added to the initial mixture to reduce the generated H<sub>2</sub>O<sub>2</sub> in this reaction. The ratio of the fluorescence intensity peak of TGA-QD over BA-QD  $(F_{TGA-QD}/F_{BA-QD})$  can be used to determine the QD fluorescent probe response from 100 to 1000  $\mu$ M glucose in vitro in TES buffer (Figure 2D). Together our results indicate that BA-QD respond to glucose in vitro, whereas the TGA-QD acts as an internal reference control remaining invariant to glucose.

We further determined the temporal patterns of QD fluorescent probe incubation with glucose on the QD fluorescence emission intensity. Figure 2E shows the fluorescence of TGA-QD remains relatively constant over the 2 h incubation period in the presence of different concentrations of glucose. Compared to TGA-QD, the BA-QD exhibits a significant and steady fluorescence quenching in the presence of glucose reaching a plateau after 60 min of reaction time (Figure 2F). This reaction time is shorter than other sensing systems such as gold NNPs requiring about 200 min. The reaction time previously reported for QD probes for glucose is about 1 h, similar to our QD glucose probe. The reaction time proviously reported for QD probes for glucose is about 1 h, similar to our QD glucose probe.

Selectivity is also a critical parameter to evaluate the performance of a fluorescent probe. We studied the fluorescence response of BA-QD to potential interfering sugars, including glucose, sucrose, fructose, lactose, galactose, and maltose. These sugars (1000  $\mu$ M, 60 min incubation) have very little effect on the BA-QD fluorescence quenching except for glucose (Figure 2G). This is in agreement with previous studies showing that glucose but not other common sugars

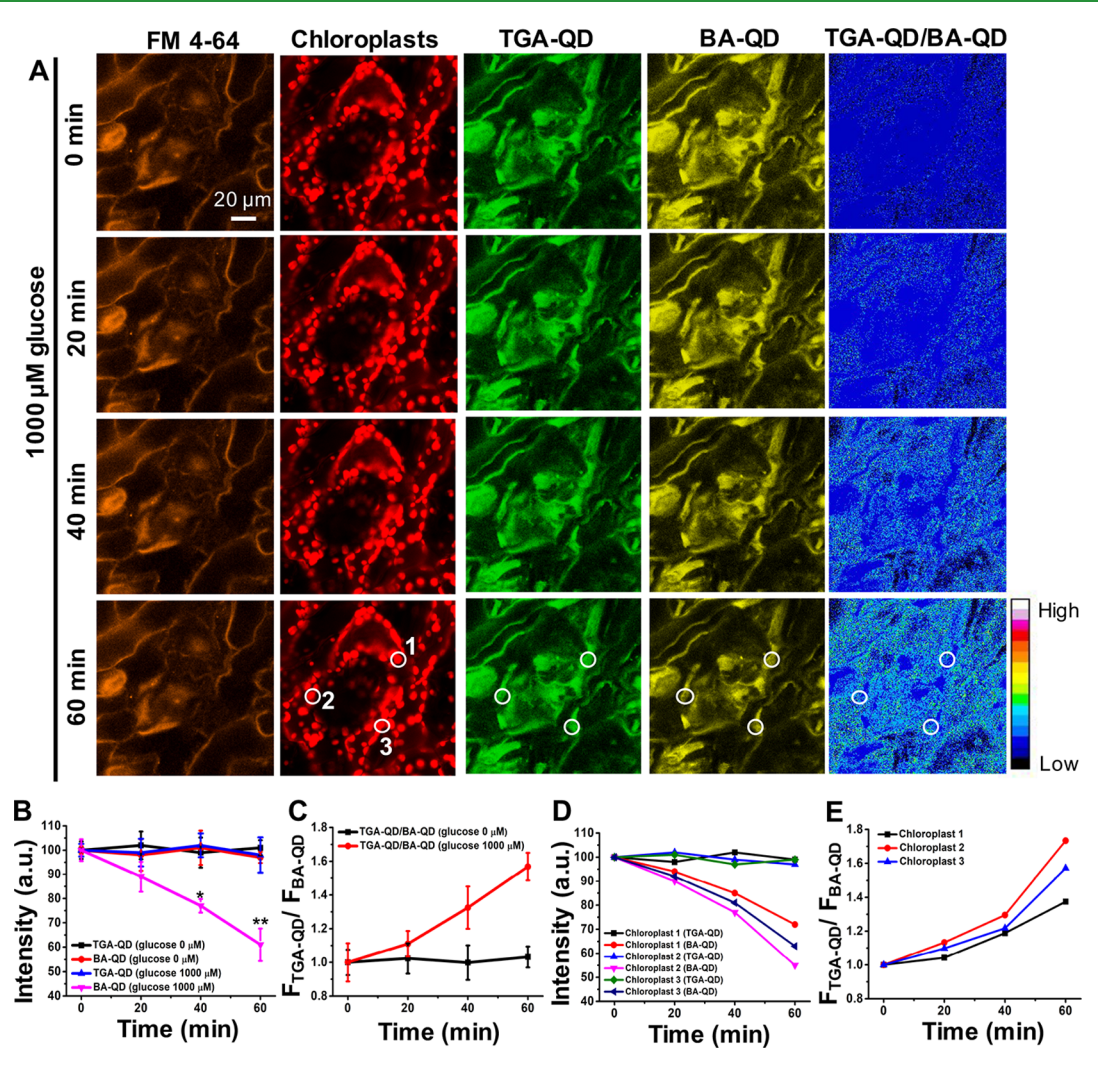


Figure 4. Glucose sensing in vivo in *Arabidopsis* photosynthetic tissues by the QD fluorescent probe. (A) Confocal images of leaf tissues stained by FM4-64 (orange, cell membrane), chloroplast pigment autofluorescence (red), TGA-QD (green), and BA-QD (yellow). After addition of glucose (1000 μM) to *Arabidopsis* leaf mesophyll cells, the fluorescence of TGA-QD remains relatively constant, whereas the fluorescence of BA-QD quenches steadily over time. Scale bar: 20 μm. (B) Temporal changes in relative fluorescence intensity of TGA-QD and BA-QD probes in the presence of 0 and 1000 μM glucose. (C) Steady increase in the ratio of TGA-QD and BA-QD fluorescence intensity ( $F_{TGA-QD}/F_{BA-QD}$ , F: fluorescence) over time. (D) Similar relative fluorescence intensity patterns were observed in randomly selected chloroplasts for TGA-QD and BA-QD, and (E) ratio of TGA-QD and BA-QD fluorescence intensity ( $F_{TGA-QD}/F_{BA-QD}/F_{BA-QD}$ ). Asterisks denote significant differences between 0 and 1000 μM glucose (t-test).

caused quenching of BA-conjugated NNPs.  $^{18,60-62}$  The BA-QD fluorescence quenching is based on the cross-linking effect with glucose by the unique reaction between BA groups on the surface of BA-QD and two pairs of cis-diols on glucose. Other sugars such as fructose, galactose, and mannose having only one pair of cis-diols with no additional cis conformational diol unit do not lead to the aggregation of BA-QD and corresponding fluorescence quenching.  $^{44}$  The existence of two pairs of cis-diols in glucose is the key structural feature that confers BA-QD a glucose-specific response.  $^{62}$  Figure 2H shows a significant increase in the ratio of  $F_{\rm TGA-QD}/F_{\rm BA-QD}$  in vitro in the presence of glucose but not for sucrose, fructose, lactose, maltose, and galactose.

DLS and TEM analysis indicate BA-QD aggregation after adding glucose because of the reaction between BA group on the surface of BA-QD and two pairs of cis-diols on glucose (Figure 2I–K). The DLS hydrodynamic diameter measurements show that BA-QD does not aggregate in water, whereas there is a significant increase in the assembly of BA-QD in the

presence of glucose (1000  $\mu$ M) (Figure 2I). Upon the addition of glucose to the BA-QD, the average DLS value increased gradually within 1 h of reaction time until an equilibrium state was reached. To examine the morphology of the glucosemediated assembly of the BA-QD, TEM was used to image the BA-QD in the absence and presence of glucose (1000  $\mu$ M) after 60 min incubation. In the absence of glucose, the BA-QD remains dispersed as a single NNP on the TEM grid (Figure 2J). After adding glucose to BA-QD, the glucose-induced assembly of BA-QD was observed in TEM images (Figure 2K), further confirming that glucose can lead to the assembly of BA-QD and consequent fluorescence quenching. The fluorescence quenching of QDs upon aggregation can be explained by exciton energy transfer and electron coupling between QDs. 63,64 Energy transfer occurs during the migration of excitons from higher to lower band gap QDs in close proximity (<10 nm). 64,65 Electronic coupling is mediated by the hybridization of band edge orbitals between neighboring QDs.<sup>66</sup>

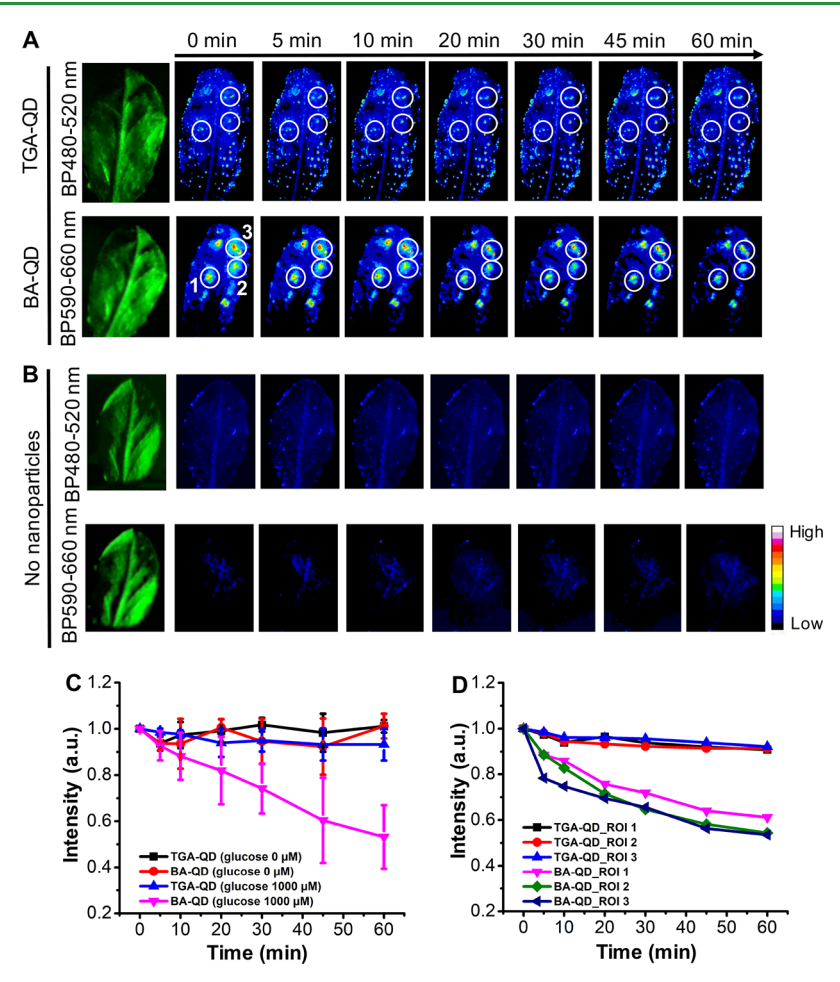


Figure 5. Standoff detection of glucose in Arabidopsis leaves using the QD fluorescent probe. (A) TGA-QD and BA-QD fluorescence signals were monitored by two Raspberry Pi cameras equipped with band pass optical filters (BP 480-520 nm and BP 590-660 nm for TGA-QD and BA-QD, respectively). The QD fluorescence emission was recorded under UV excitation of 365 nm and 10 s exposure time. (B) Background fluorescence signal from leaf without NNPs. (C) Temporal patterns of BA-QD and TGA-QD fluorescence intensity from 0 to 60 min after adding glucose (1000  $\mu M$ ) and without glucose (0  $\mu M$ ) for whole leaf and (D) selected regions of interest. Mean  $\pm$  SD.

3.3. In Vivo Glucose Sensing by a QD Fluorescent Probe in Photosynthetic Organisms. We detected the presence of glucose in the algae C. zeylanica by confocal microscopy using the QD probe fluorescence emission. Confocal images showed that the QD probe enters into the algae cell cytosol after 2 h incubation (Figure 3A). A strong fluorescence signal can be observed from TGA-QD and BA-QD channels before adding glucose to the algae in water. Upon increasing incubation time of algae cells with glucose at 1000 μM concentration, the fluorescence signal from TGA-QD remain constant and strong, whereas BA-QD fluorescence decreases gradually indicating aggregation of BA-QD (Figure 3B,C). The quenching of BA-QD is not significant at concentrations of glucose below 200 µM after 60 min incubation time (Figures 3C and S3-S5). The QD probe can detect glucose in living algae when the concentration of glucose is 500  $\mu$ M after 40 min incubation (Figure S6). The ratio of  $F_{\rm TGA\text{-}QD}/F_{\rm BA\text{-}QD}$  increases linearly with time at glucose concentrations of 500 and 1000  $\mu$ M (Figure 3D). No cell damage in algae incubated with TGA-QD and BA-QD (200 nM) was observed after 24 h (Figure S7A).

We also used Arabidopsis, one of the most well-studied model plant species, as a system to demonstrate the detection of glucose by the QD probe in vivo (Figures 4 and S8). We infiltrated the QD probe (TGA-QD and BA-QD) through the

lamina of Arabidopsis leaves, allowing 2 h incubation before confocal imaging. Similarly, no cell damage nor changes in chlorophyll content index in Arabidopsis leaves were observed after 24 h incubation with TGA-QD and BA-QD (200 nM) (Figure S7B,C). Without glucose addition, the fluorescence signal of TGA-QD and BA-QD does not change after 60 min observation in excised leaves (Figures 4A,B and S8). In contrast, adding 1000 µM glucose to Arabidopsis leaf mesophyll cells leads to the gradual decrease of BA-QD fluorescence intensity, whereas the fluorescence intensity of TGA-QD remains relatively constant (Figure 4A,B). The gradual increase in the ratio between the fluorescence intensity of TGA-QD and BA-QD  $(F_{TGA-QD}/F_{BA-QD})$  reflects the interaction of the QD probe with glucose in Arabidopsis leaves (Figure 4A,C). The overlay between TGA-QD and BA-QD confocal images in algae and Arabidopsis indicates a highly even distribution of these two QDs in vivo (Figure S9). The TGA-QD and BA-QD distribution patterns in leaf mesophyll cells have an average overlay rate from 86.9  $\pm$  2.0% to 89.4  $\pm$ 3.9% over the duration of the experiments (Figure S9D). No significant difference of colocalization rate with chloroplasts in Arabidopsis plants was found between TGA-QD and BA-QD (Figure S10A,B). The similar subcellular localization of TGA-QD and BA-QD in leaf mesophyll cells and chloroplasts indicates that this QD ratiometric approach is adequate for

monitoring glucose levels at scales ranging from organelles, tissues to whole leaves. Metabolite FRET nanosensors have been successfully used to characterize and monitor glucose in yeast and in *Arabidopsis*. <sup>14,67</sup> However, the detection of glucose has been challenging in nonmodel plant systems because it requires the use of mutants or coexpression of the FRET nanosensor. <sup>28</sup> Compared to metabolite FRET nanosensors, the QD probe does not require special genetic modification for glucose sensing in plants. Thus, this plant nanobiotechnology approach for detecting glucose has the potential to be translated from model organisms to wild-type photosynthetic organisms.

Chloroplasts, the main plant organelles responsible for energy harvesting and conversion,<sup>68</sup> use energy from sunlight to convert carbon dioxide and water into energy-rich organic molecules, such as glucose.<sup>69</sup> Glucose plays a key role as a signaling molecule in plants, controlling several aspects of plant physiology and development.<sup>2,5</sup> Detection of glucose within subcellular compartments is important for understanding its role as a signaling molecule.<sup>5</sup> The QD probe has the spatial resolution for detecting glucose in single chloroplast of Arabidopsis leaf mesophyll cells (Figure 4D,E). Three chloroplasts were chosen randomly for monitoring the fluorescence intensity changes in TGA-QD and BA-QD in leaf mesophyll confocal images (Figure 4A). As expected, the fluorescence intensity of TGA-QD remains stable after 60 min incubation (Figure 4D). In contrast, the fluorescence of BA-QD quenches rapidly. The increase in intensity of  $F_{\rm TGA\text{-}QD}/$  $F_{\text{BA-QD}}$  ratio maps indicated glucose detection by the QD probe in single chloroplast after glucose addition (Figure 4E). Without addition of glucose, the ratio of fluorescence intensity between TGA-QD and BA-QD does not change significantly in single chloroplasts exposed to light (Figure S11). The subcellular resolution of our QD glucose probe has potential applications in tracking glucose production and transport within cells, tissues, or whole leaves. Understanding the spatial distribution of glucose in plant cells is fundamental to dissect its role in signaling transduction and regulation of plant growth and reproduction. 70 Our results indicate that besides chloroplasts, the highest increase in  $F_{TGA-OD}/F_{BA-OD}$  signals is in the vacuole (Figure 4A), in agreement with previous studies. As the site of glucose synthesis, chloroplasts are expected to exhibit the largest changes in glucose levels under dark conditions. 12 NNP glucose sensing approaches with high spatial resolution will significantly improve our understanding of the role of this key signaling molecule in planta. Together these results indicate that glucose can be detected at the single chloroplast level in living photosynthetic tissues by using the OD probe developed in this study.

3.4. In Vivo Standoff Imaging of BA-QD Fluorescence Changes in Response to Glucose in Plant Leaves. To monitor glucose in vivo in whole leaves of *Arabidopsis* plants, we created a Raspberry Pi camera system that images and records the visible fluorescence signal of BA-QD and TGA-QD in the presence of glucose (Figure 5). The Raspberry Pi camera system is a low-cost and robust approach to image NNP fluorescence signals in planta. After topical delivery of glucose (1000  $\mu$ M) to the leaf lamina, the fluorescence emission of TGA-QD from dark-adapted *Arabidopsis* leaves is relatively stable from 0 to 60 min (Figure 5A,C), whereas the BA-QD fluorescence decreases by 53% (P < 0.001) (Figure 5A,C). A similar response of QD fluorescence signal was found in three selected regions of the leaf lamina (Figure 5D). Leaves

without NNPs exhibited a low and stable background signal within the selected QD fluorescence emission after applying glucose (Figure 5B). In experiments, without the addition of glucose, reductions of BA-QD fluorescence intensity are observed in leaves under dark compared with stable TGA-QD fluorescence signals (Figure S12A,C). However, the BA-QD fluorescence intensity changes are relatively lower and not homogeneous compared with leaves exposed to 1000 µM glucose. No significant changes of BA-QD and TGA-QD fluorescence signal were found in Arabidopsis leaves under light (200  $\mu$ mol m<sup>-2</sup> s<sup>-1</sup>) except at the leaf tip where light-driven evapotranspiration could have promoted the movement of QD (Figure S12B,D). <sup>74,75</sup> Together, these results point out that the QD glucose probe is well suited to monitor glucose under dark when chloroplasts are synthesizing and exporting glucose, and there is no evapotranspiration. Overall, our results demonstrate that imaging a QD probe by a Raspberry Pi camera system is a practical tool for monitoring glucose in plant leaves. This in vivo standoff QD glucose imaging approach has the potential to be utilized for directly monitoring changes in glucose levels of photosynthetic organisms in the field.

#### 4. CONCLUSIONS

We developed an in vivo standoff glucose imaging system based on a QD fluorescent probe designed for photosynthetic tissues. The TGA-QD acts as a reference fluorescence probe which does not respond to glucose, whereas the BA-QD fluorescence successfully monitors the presence of glucose above 100 and 500  $\mu$ M in vitro and in vivo. To our knowledge, the starting analytical range of in vivo glucose QD detection has been reported to be within  $100-400 \mu M$ . Glucose levels in photosynthetic tissues of light-grown plants have been estimated to range between 300 and 2000  $\mu$ M. Thus, the BA-QDs synthesized in this study are within the reported sensitivity range of glucose detection of 500  $\mu$ M (in planta). The ratio of  $F_{\rm TGA\text{-}QD}/F_{\rm BA\text{-}QD}$  can be used to detect glucose in vivo both in algae and land plants such as Arabidopsis within this physiological range. The unique glucose-mediated assembly and fluorescence quenching of BA-QD enable a selective response to glucose against other common sugars in plants such as maltose, fructose, galactose, and sucrose. The response of the QD fluorescent probe in algae and Arabidopsis plants in vivo was similar to in vitro tests corroborating the robustness of the QD-based ratiometric approach for biological research applications. Previously reported in vivo glucose sensing approaches in plants require genetic modification. <sup>13–15,28</sup> Therefore, they are not currently practical tools for enabling in vivo standoff detection of glucose in nonmodel plant species. In contrast with laboratory-based methods, our portable QD glucose sensing approach has the potential of allowing research in nonmodel plant species both in the laboratory and the field. This QD-based probe for in vivo standoff imaging is a highly enabling tool for glucose sensing in solar energy conversion biomaterials and photosynthesis research.

# ASSOCIATED CONTENT

#### Supporting Information

The Supporting Information is available free of charge on the ACS Publications website at DOI: 10.1021/acsami.8b07179.

Characterization of TGA-QD and BA-QD; in vitro detection of glucose and reversibility of QD fluorescent

probe in TES buffer; confocal images of QD glucose probe fluorescence intensity in algae (C. zeylanica) under no glucose and 100, 200, and 500  $\mu$ M glucose addition (0, 20, 40, and 60 min); cell viability staining of algae and Arabidopsis incubated with TGA-QD and BA-QD; confocal images of leaf mesophyll cells of Arabidopsis plants incubated with QD fluorescent probe under control conditions of no glucose (0  $\mu$ M); TGA-QD and BA-QD spatial distribution in algae and in Arabidopsis leaf mesophyll cells and chloroplasts; fluorescence intensity changes of QD glucose probe in single chloroplasts of Arabidopsis; and standoff imaging of TGA-QD and BA-QD fluorescence signal in Arabidopsis leaves under dark and light (200  $\mu$ mol m<sup>-2</sup> s<sup>-1</sup>) (PDF)

#### AUTHOR INFORMATION

## **Corresponding Author**

\*E-mail: juanpablo.giraldo@ucr.edu.

#### ORCID ®

Juan Pablo Giraldo: 0000-0002-8400-8944

#### **Present Address**

<sup>†</sup>College of Biophotonics, South China Normal University, Guangzhou 510631, China.

#### **Author Contributions**

<sup>‡</sup>J.L. and H.W. contributed equally to this paper. J.P.G., J.L., and H.W. conceived and designed this study. J.L., H.W., I.S., and M.F. performed experiments. J.L., H.W., and J.P.G. analyzed the results. J.P.G., H.W., and J.L. wrote the manuscript.

# Notes

The authors declare no competing financial interest.

# ACKNOWLEDGMENTS

This work was supported by a seed grant from the University of California, Riverside, and USDA NIFA Hatch project no. 1009710. This material is based upon the work supported by the National Science Foundation under grant no. 1817363.

#### REFERENCES

- (1) Libessart, N.; Maddelein, M. L.; Van Den Koornhuyse, N.; Decq, A.; Delrue, B.; Mouille, G.; D'Hulst, C.; Ball, S. Storage, Photosynthesis, and Growth: The Conditional Nature of Mutations Affecting Starch Synthesis and Structure in Chlamydomonas. *Plant Cell* **1995**, *7*, 1117–1127
- (2) Moore, B.; Zhou, L.; Rolland, F.; Hall, Q.; Cheng, W. H.; Liu, Y. X.; Hwang, I.; Jones, T.; Sheen, J. Role of the *Arabidopsis* Glucose Sensor HXK1 in Nutrient, Light, and Hormonal Signaling. *Science* **2003**, *300*, 332–336.
- (3) Niittyla, T.; Messerli, G.; Trevisan, M.; Chen, J.; Smith, A. M.; Zeeman, S. C. A Previously Unknown Maltose Transporter Essential for Starch Degradation in Leaves. *Science* **2004**, *303*, 87–89.
- (4) Grootegoed, J. A.; Jansen, R.; Van Der Molen, H. J. The Role of Glucose, Pyruvate and Lactate in ATP Production by Rat Spermatocytes and Spermatids. *Biochim. Biophys. Acta* **1984**, *767*, 248–256.
- (5) Rolland, F.; Baena-Gonzalez, E.; Sheen, J. Sugar Sensing and Signaling in Plants: Conserved and Novel Mechanisms. *Annu. Rev. Plant Biol.* **2006**, *57*, *675*–709.
- (6) Zhou, L.; Jang, J.-c.; Jones, T. L.; Sheen, J. Glucose and Ethylene Signal Transduction Crosstalk Revealed by an Arabidopsis Glucose-Insensitive Mutant. *Proc. Natl. Acad. Sci. U.S.A.* **1998**, 95, 10294–10299.

- (7) Lawlor, D. W.; Cornic, G. Photosynthetic Carbon Assimilation and Associated Metabolism in Relation to Water Deficits in Higher Plants. *Plant. Cell Environ.* **2002**, *25*, 275–294.
- (8) Giraldo, J. P.; Wheeler, J. K.; Huggett, B. A.; Holbrook, N. M. The Role of Leaf Hydraulic Conductance Dynamics on the Timing of Leaf Senescence. *Funct. Plant Biol.* **2014**, *41*, 37–47.
- (9) Tanaka, Y.; Sugano, S. S.; Shimada, T.; Hara-Nishimura, I. Enhancement of Leaf Photosynthetic Capacity through Increased Stomatal Density in Arabidopsis. *New Phytol.* **2013**, *198*, 757–764.
- (10) Wu, H.; Shabala, L.; Shabala, S.; Giraldo, J. P. Hydroxyl Radical Scavenging by Cerium Oxide Nanoparticles Improves *Arabidopsis* Salinity Tolerance by Enhancing Leaf Mesophyll Potassium Retention. *Environ. Sci. Nano* **2018**, *5*, 1567.
- (11) Wu, H.; Tito, N.; Giraldo, J. P. Anionic Cerium Oxide Nanoparticles Protect Plant Photosynthesis from Abiotic Stress by Scavenging Reactive Oxygen Species. *ACS Nano* **2017**, *11*, 11283–11297
- (12) Fehr, M.; Frommer, W. B.; Lalonde, S. Visualization of Maltose Uptake in Living Yeast Cells by Fluorescent Nanosensors. *Proc. Natl. Acad. Sci. U.S.A.* **2002**, *99*, 9846–9851.
- (13) Deuschle, K.; Chaudhuri, B.; Okumoto, S.; Lager, I.; Lalonde, S.; Frommer, W. B. Rapid Metabolism of Glucose Detected with FRET Glucose Nanosensors in Epidermal Cells and Intact Roots of *Arabidopsis* RNA-Silencing Mutants. *Plant Cell* **2006**, *18*, 2314–2325.
- (14) Chaudhuri, B.; Hörmann, F.; Lalonde, S.; Brady, S. M.; Orlando, D. A.; Benfey, P.; Frommer, W. B. Protonophore- and PH-Insensitive Glucose and Sucrose Accumulation Detected by FRET Nanosensors in Arabidopsis Root Tips. *Plant J.* **2008**, *56*, 948–962.
- (15) Zhu, Q.; Wang, L.; Dong, Q.; Chang, S.; Wen, K.; Jia, S.; Chu, Z.; Wang, H.; Gao, P.; Zhao, H.; Han, S.; Wang, Y. FRET-Based Glucose Imaging Identifies Glucose Signalling in Response to Biotic and Abiotic Stresses in Rice Roots. *J. Plant Physiol.* **2017**, 215, 65–72.
- (16) Tang, Y.; Yang, Q.; Wu, T.; Liu, L.; Ding, Y.; Yu, B. Fluorescence Enhancement of Cadmium Selenide Quantum Dots Assembled on Silver Nanoparticles and Its Application to Glucose Detection. *Langmuir* **2014**, *30*, 6324–6330.
- (17) Steiner, M.-S.; Duerkop, A.; Wolfbeis, O. S. Optical Methods for Sensing Glucose. *Chem. Soc. Rev.* **2011**, *40*, 4805–4835.
- (18) Qu, Z.-b.; Zhou, X.; Gu, L.; Lan, R.; Sun, D.; Yu, D.; Shi, G. Boronic Acid Functionalized Graphene Quantum Dots as a Fluorescent Probe for Selective and Sensitive Glucose Determination in Microdialysate. *Chem. Commun.* **2013**, 49, 9830.
- (19) Zhang, X.; Liu, M.; Liu, H.; Zhang, S. Low-Toxic Ag2S Quantum Dots for Photoelectrochemical Detection Glucose and Cancer Cells. *Biosens. Bioelectron.* **2014**, *56*, 307–312.
- (20) Larson, D. R.; Zipfel, W. R.; Williams, R. M.; Clark, S. W.; Bruchez, M. P.; Wise, F. W.; Webb, W. W. Water-Soluble Quantum Dots for Multiphoton Fluorescence Imaging in Vivo. *Science* **2003**, 300, 1434–1436.
- (21) Michalet, X.; Pinaud, F. F.; Bentolila, L. A.; Tsay, J. M.; Doose, S.; Li, J. J.; Sundaresan, G.; Wu, A. M.; Gambhir, S. S.; Weiss, S. Quantum Dots for Live Cells, in Vivo Imaging, and Diagnostics. *Science* **2005**, *307*, 538–544.
- (22) Wu, W.; Zhou, T.; Berliner, A.; Banerjee, P.; Zhou, S. Glucose-Mediated Assembly of Phenylboronic Acid Modified CdTe/ZnTe/ZnS Quantum Dots for Intracellular Glucose Probing. *Angew. Chem., Int. Ed.* **2010**, 49, 6554–6558.
- (23) Albersheim, P.; Darvill, A.; Roberts, K.; Sederoff, R.; Staehelin, A. *Plant Cell Walls. From Chemistry to Biology*; Garland Science, 2011; pp 241–242.
- (24) Chan, W. C.; Nie, S. Quantum Dot Bioconjugates for Ultrasensitive Nonisotopic Detection. *Science* **1998**, *281*, 2016–2018. (25) Hines, D. A.; Kamat, P. V. Recent Advances in Quantum Dot Surface Chemistry. *ACS Appl. Mater. Interfaces* **2014**, *6*, 3041–3057. (26) Wu, X.; Liu, H.; Liu, J.; Haley, K. N.; Treadway, J. A.; Larson, J.
- (26) Wu, X.; Liu, H.; Liu, J.; Haley, K. N.; Treadway, J. A.; Larson, J. P.; Ge, N.; Peale, F.; Bruchez, M. P. Immunofluorescent labeling of cancer marker Her2 and other cellular targets with semiconductor quantum dots. *Nat. Biotechnol.* **2003**, *21*, 41–46.

- (27) Resch-Genger, U.; Grabolle, M.; Cavaliere-Jaricot, S.; Nitschke, R.; Nann, T. Quantum dots versus organic dyes as fluorescent labels. Methods 2008, 5, 763-775.
- (28) Chaudhuri, B.; Hormann, F.; Frommer, W. B. Dynamic Imaging of Glucose Flux Impedance Using FRET Sensors in Wild-Type Arabidopsis Plants. J. Exp. Bot. 2011, 62, 2411-2417.
- (29) Zhang, J.; Campbell, R. E.; Ting, A. Y.; Tsien, R. Y. Creating New Fluorescent Probes for Cell Biology. Nat. Rev. Mol. Cell Biol. 2002, 3, 906-918.
- (30) Wong, M. H.; Giraldo, J. P.; Kwak, S.-Y.; Koman, V. B.; Sinclair, R.; Lew, T. T. S.; Bisker, G.; Liu, P.; Strano, M. S. Nitroaromatic Detection and Infrared Communication from Wild-Type Plants Using Plant Nanobionics. Nat. Mater. 2017, 16, 264-272.
- (31) Giraldo, J. P.; Landry, M. P.; Kwak, S.-Y.; Jain, R. M.; Wong, M. H.; Iverson, N. M.; Ben-Naim, M.; Strano, M. S. A Ratiometric Sensor Using Single Chirality Near-Infrared Fluorescent Carbon Nanotubes: Application to in Vivo Monitoring. Small 2015, 11, 3973-3984.
- (32) Näreoja, T.; Deguchi, T.; Christ, S.; Peltomaa, R.; Prabhakar, N.; Fazeli, E.; Perälä, N.; Rosenholm, J. M.; Arppe, R.; Soukka, T.; Schäferling, M. Ratiometric Sensing and Imaging of Intracellular PH Using Polyethylenimine-Coated Photon Upconversion Nanoprobes. Anal. Chem. 2017, 89, 1501-1508.
- (33) Byrne, A.; Jacobs, J.; Burke, C. S.; Martin, A.; Heise, A.; Keyes, T. E. Rational Design of Polymeric Core Shell Ratiometric Oxygen-Sensing Nanostructures. Analyst 2017, 142, 3400-3406.
- (34) Heller, D. A.; Jin, H.; Martinez, B. M.; Patel, D.; Miller, B. M.; Yeung, T.-K.; Jena, P. V.; Höbartner, C.; Ha, T.; Silverman, S. K.; Strano, M. S. Multimodal Optical Sensing and Analyte Specificity Using Single-Walled Carbon Nanotubes. Nat. Nanotechnol. 2009, 4, 114-120.
- (35) Clegg, R. M. Fluorescence Resonance Energy Transfer. Curr. Opin. Biotechnol. 1995, 6, 103-110.
- (36) Shen, P.; Xia, Y. Synthesis-Modification Integration: One-Step Fabrication of Boronic Acid Functionalized Carbon Dots for Fluorescent Blood Sugar Sensing. Anal. Chem. 2014, 86, 5323-5329.
- (37) Cordes, D. B.; Gamsey, S.; Singaram, B. Fluorescent Quantum Dots with Boronic Acid Substituted Viologens to Sense Glucose in Aqueous Solution. Angew. Chem., Int. Ed. 2006, 45, 3829-3832.
- (38) Mader, H. S.; Wolfbeis, O. S. Boronic Acid Based Probes for Microdetermination of Saccharides and Glycosylated Biomolecules. Microchim. Acta 2008, 162, 1-34.
- (39) Zhang, L.; Zhang, Z.-Y.; Liang, R.-P.; Li, Y.-H.; Qiu, J.-D. Boron-Doped Graphene Quantum Dots for Selective Glucose Sensing Based on the "Abnormal" Aggregation-Induced Photoluminescence Enhancement. Anal. Chem. 2014, 86, 4423-4430.
- (40) Hall, D. G. Structure, Properties, and Preparation of Boronic Acid Derivatives. Boronic Acids; Wiley-VCH Verlag GmbH & Co. KGaA: Weinheim, Germany, 2011; pp 1-133.
- (41) James, T. D.; Sandanayake, K. R. A. S.; Shinkai, S. Saccharide Sensing with Molecular Receptors Based on Boronic Acid. Angew. Chem., Int. Ed. Engl. 1996, 35, 1910-1922.
- (42) Kuivila, H. G.; Keough, A. H.; Soboczenski, E. J. Areneboronates from diols and polyols. J. Org. Chem. 1954, 19, 780-783.
- (43) Fang, H.; Kaur, G.; Wang, B. Progress in Boronic Acid-Based Fluorescent Glucose Sensors. J. Fluoresc. 2004, 14, 481-489.
- (44) Liu, Y.; Deng, C.; Tang, L.; Qin, A.; Hu, R.; Sun, J. Z.; Tang, B. Z. Specific Detection ofd-Glucose by a Tetraphenylethene-Based Fluorescent Sensor. J. Am. Chem. Soc. 2011, 133, 660-663.
- (45) Heineke, D.; Wildenberger, K.; Sonnewald, U.; Willmitzer, L.; Heldt, H. Accumulation of Hexoses in Leaf Vacuoles: Studies with Transgenic Tobacco Plants Expressing Yeast-Derived Invertase in the Cytosol, Vacuole or Apoplasm. Planta 1994, 194, 29-33.
- (46) Xu, J.; Li, J.; Lin, S.; Wu, T.; Huang, H.; Zhang, K.; Sun, Y.; Yeung, K. W. K.; Li, G.; Bian, L. Nanocarrier-Mediated Codelivery of Small Molecular Drugs and SiRNA to Enhance Chondrogenic Differentiation and Suppress Hypertrophy of Human Mesenchymal Stem Cells. Adv. Funct. Mater. 2016, 26, 2463-2472.

- (47) Li, J.; Lee, W. Y.; Wu, T.; Xu, J.; Zhang, K.; Li, G.; Xia, J.; Bian, L. Multifunctional Quantum Dot Nanoparticles for Effective Differentiation and Long-Term Tracking of Human Mesenchymal Stem Cells In Vitro and In Vivo. Adv. Healthcare Mater. 2016, 5, 1049-
- (48) Wu, H.; Santana, I.; Dansie, J.; Giraldo, J. P. In Vivo Delivery of Nanoparticles into Plant Leaves. Curr. Protoc. Chem. Biol. 2017, 9, 269-284.
- (49) Hauser, M.; Eichelmann, H.; Heber, U.; Laisk, A. Chloroplast PH Values and Buffer Capacities in Darkened Leaves as Revealed by CO2 Solubilization in Vivo. Planta 1995, 196, 199-204.
- (50) Gout, E.; Bligny, R.; Douce, R. Regulation of Intracellular pH Values in Higher Plant Cells. Carbon-13 and Phosphorus-31 Nuclear Magnetic Resonance Studies. J. Biol. Chem. 1992, 267, 13903-13909.
- (51) Manders, E. M. M. Chromatic Shift in Multicolour Confocal Microscopy. J. Microsc. 1997, 185, 321-328.
- (52) Bolte, S.; Cordelières, F. P. A Guided Tour into Subcellular Colocalisation Analysis in Light Microscopy. J. Microsc. 2006, 224,
- (53) Tong, Z.; Rajeev, G.; Guo, K.; Ivask, A.; McCormick, S.; Lombi, E.; Priest, C.; Voelcker, N. H. Microfluidic Cell Microarray Platform for High Throughput Analysis of Particle-Cell Interactions. Anal. Chem. 2018, 90, 4338-4347.
- (54) Newkirk, G. M.; Wu, H.; Santana, I.; Giraldo, J. P. Catalytic Scavenging of Plant Reactive Oxygen Species in Vivo by Anionic Cerium Oxide Nanoparticles. J. Visualized Exp. 2018, DOI: 10.3791/ 58373.
- (55) Wu, H.; Shabala, L.; Zhou, M.; Stefano, G.; Pandolfi, C.; Mancuso, S.; Shabala, S. Developing and Validating a High-Throughput Assay for Salinity Tissue Tolerance in Wheat and Barley. Planta 2015, 242, 847-857.
- (56) Bao, H.; Gong, Y.; Li, Z.; Gao, M. Enhancement Effect of Illumination on the Photoluminescence of Water-Soluble CdTe Nanocrystals: Toward Highly Fluorescent CdTe/CdS Core-Shell Structure. Chem. Mater. 2004, 16, 3853-3859.
- (57) Treibitz, T.; Neal, B. P.; Kline, D. I.; Beijbom, O.; Roberts, P. L. D.; Mitchell, B. G.; Kriegman, D. Wide Field-of-View Fluorescence Imaging of Coral Reefs. Sci. Rep. 2015, 5, 1-9.
- (58) Peng, Z. A.; Peng, X. Formation of High-Quality CdTe, CdSe, and CdS Nanocrystals Using CdO as Precursor. J. Am. Chem. Soc. 2001, 123, 183-184.
- (59) Wang, Q.; Yang, L.; Yang, X.; Wang, K.; Liu, J. Use of Mercaptophenylboronic Acid Functionalized Gold Nanoparticles in a Sensitive and Selective Dynamic Light Scattering Assay for Glucose Detection in Serum. Analyst 2013, 138, 5146.
- (60) Nair, P. A.; Sreenivasan, K. Non enzymatic colorimetric detection of glucose using cyanophenyl boronic acid included  $\beta$ cyclodextrin stabilized gold nanoparticles. Anal. Methods 2016, 8,
- (61) Naaz, S.; Poddar, S.; Bayen, S. P.; Mondal, M. K.; Roy, D.; Mondal, S. K.; Chowdhury, P.; Saha, S. K. Tenfold Enhancement of Fluorescence Quantum Yield of Water Soluble Silver Nanoclusters for Nano-Molar Level Glucose Sensing and Precise Determination of Blood Glucose Level. Sens. Actuators, B 2018, 255, 332-340.
- (62) Hao, T.; Wei, X.; Nie, Y.; Xu, Y.; Lu, K.; Yan, Y.; Zhou, Z. Surface Modification and Ratiometric Fluorescence Dual Function Enhancement for Visual and Fluorescent Detection of Glucose Based on Dual-Emission Quantum Dots Hybrid. Sens. Actuators, B 2016, 230, 70-76.
- (63) Noh, M.; Kim, T.; Lee, H.; Kim, C.-K.; Joo, S.-W.; Lee, K. Fluorescence Quenching Caused by Aggregation of Water-Soluble CdSe Quantum Dots. Colloids Surf., A 2010, 359, 39-44.
- (64) Kang, T.; Um, K.; Park, J.; Chang, H.; Lee, D. C.; Kim, C.-K.; Lee, K. Minimizing the Fluorescence Quenching Caused by Uncontrolled Aggregation of CdSe/CdS Core/Shell Quantum Dots for Biosensor Applications. Sens. Actuators, B 2016, 222, 871-878.
- (65) Wu, M.; Mukherjee, P.; Lamont, D. N.; Waldeck, D. H. Electron Transfer and Fluorescence Quenching of Nanoparticle Assemblies. J. Phys. Chem. C 2010, 114, 5751-5759.

- (66) Koole, R.; Liljeroth, P.; de Mello Donegá, C.; Vanmaekelbergh, D.; Meijerink, A. Electronic Coupling and Exciton Energy Transfer in CdTe Quantum-Dot Molecules. *J. Am. Chem. Soc.* **2006**, *128*, 10436—10441.
- (67) Bermejo, C.; Haerizadeh, F.; Takanaga, H.; Chermak, D.; Frommer, W. B. Dynamic Analysis of Cytosolic Glucose and ATP Levels in Yeast Using Optical Sensors. *Biochem. J.* **2010**, *432*, 399–406
- (68) Lichtenthaler, H. K.; Buschmann, C.; Döll, M.; Fietz, H.-J.; Bach, T.; Kozel, U.; Meier, D.; Rahmsdorf, U. Photosynthetic Activity, Chloroplast Ultrastructure, and Leaf Characteristics of High-Light and Low-Light Plants and of Sun and Shade Leaves. *Photosynth. Res.* 1981, 2, 115–141.
- (69) Arnon, D. I.; Allen, M. B.; Whatley, F. R. Photosynthesis by Isolated Chloroplasts. *Nature* **1954**, *174*, 394–396.
- (70) Eveland, A. L.; Jackson, D. P. Sugars, Signalling, and Plant Development. *J. Exp. Bot.* **2012**, *63*, 3367–3377.
- (71) Farre, E. M.; Tiessen, A.; Roessner, U.; Geigenberger, P.; Trethewey, R. N.; Willmitzer, L. Analysis of the Compartmentation of Glycolytic Intermediates, Nucleotides, Sugars, Organic Acids, Amino Acids, and Sugar Alcohols in Potato Tubers Using a Nonaqueous Fractionation Method. *Plant Physiol.* **2001**, *127*, 685–700.
- (72) Servaites, J. C.; Geiger, D. R. Kinetic Characteristics of Chloroplast Glucose Transport. J. Exp. Bot. 2002, 53, 1581–1591.
- (73) Ĝiraldo, J. P.; Landry, M. P.; Faltermeier, S. M.; McNicholas, T. P.; Iverson, N. M.; Boghossian, A. A.; Reuel, N. F.; Hilmer, A. J.; Sen, F.; Brew, J. A.; Strano, M. S. Plant Nanobionics Approach to Augment Photosynthesis and Biochemical Sensing. *Nat. Mater.* **2014**, *13*, 400–408
- (74) Tang, H.; Dubayah, R. Light-Driven Growth in Amazon Evergreen Forests Explained by Seasonal Variations of Vertical Canopy Structure. *Proc. Natl. Acad. Sci. U.S.A.* **2017**, *114*, 2640–2644.
- (75) Cramer, M. D.; Hoffmann, V.; Verboom, G. A. Nutrient availability moderates transpiration in Ehrharta calycina. *New Phytol.* **2008**, *179*, 1048–1057.